Journal of Thermal Analysis and Calorimetry, Vol. 61 (2000) 273–287

PLASMA TECHNOLOGIES FOR REDUCING CO_2 EMISSIONS FROM COMBUSTION EXHAUST WITH TOXIC ADMIXTURES TO UTILISABLE PRODUCTS*

M. Morvová, F. Hanic and I. Morva

Institute of Physics, Faculty of Mathematics and Physics, Comenius University
Mlynská Dolina F2, SR-842 15 Bratislava, Slovakia

Abstract

The method reported here provides a contribution to CO_2 and combustion exhaust utilisation. A multifunctional system for gas removal was tested on various sources of exhaust (internal combustion engine, brown coal boiler, bituminous pulverised coal boiler, gas boiler, glass oven, VOC sources) in full-scale or by-pass gas flow volumes.

A spontaneously-pulsing, direct-current electric discharge operating in a corona geometry was used. The discharge has strongly shining channels migrating quickly along the stressed electrode. The synergetic effect of electric discharge and heterogeneous catalysis on the organometallic part of the product formed on the non-stressed electrode was responsible for the specific character of the products. The final product of the process is a powder with a fractal structure on the microscopic level with low specific mass and insoluble in water. The main component (95%) of the solid product is an amorphous condensate of amino acids with about 5% of organometallic compound with catalytic properties. The product was analysed using IR absorption spectrometry, microscopic photography, HPLC and thermogravimetry. The following amino acids were observed in the final product: alanine, serine, glycine, aspartic acid, lysine, arginine, methionine, histidine.

Keywords: amino acids, CO_2 utilisation, electric discharge, exhaust gas cleaning, nitrogen fixation, origin of life on Earth, oxamidato complexes, tetra-pyrrole complexes

Introduction

Up to 85% of all forms of energy (electricity and heat production, industry and transport) is produced in combustion processes. This was the reason for focussing our attention on the creation of multifunctional equipment for combustion exhaust cleaning.

Real combustion exhaust contains between 800 and 2 000 various compounds, including free-radicals, excited molecules produced by the combustion process. In addition to the main combustion components, CO_2, water and nitrogen, the following components usually participate in the exhaust gases: carbon monoxide, nitrogen oxides, hydrocarbons (olefines, aldehydes, VOC, semi-VOC, PAH, nitro-PAH, acro-

* Dedicated to Prof. Šesták in recognition of his outstanding activity in thermal analysis

1418–2874/2000/ $ 5.00

Akadémiai Kiadó, Budapest
Kluwer Academic Publishers, Dordrecht

leins, dioxines), particulates (the size mainly about 0.2 μm containing carbon, metal oxides, nitrate and sulfate compounds) [1].

Global warming, ozone depletion, acid rain and smog are pre-eminent environmental problems facing the world today. Much of the current concern about the fate of the global environment is related to the increased concentration of greenhouse gases, because they trap infrared radiation. Carbon dioxide is the single most important greenhouse gas. Methane, carbon monoxide and dinitrogen oxide have about the same effect as carbon dioxide, but their concentrations in the atmosphere are about three orders of magnitude lower [2]. To protect the climate and ecosystem for present and future generations it is necessary to reduce the present emission level of CO_2, as was agreed in Kyoto (1997).

Non-thermal plasma techniques offer an innovative approach to the solution of some of these problems. The mean electron energy in a non-thermal plasma is considerably higher than that of the components of the ambient gas. A non-thermal plasma can also be produced in a corona discharge.

A corona discharge can exist in various forms in a non-uniform gap, such as a wire-cylinder or a point-to-plane geometry and can be operated under dc, ac or pulsed conditions. When a dielectric material is present between the electrodes, the discharge is known as silent, barrier, partial. In special situations, the discharge is propagated on the surface of the dielectric material. Such a surface discharge can occur in a corona discharge after surface modification of electrodes.

One of the most important uses of a corona discharge is in an electrostatic precipitator. This application is very important from the environmental point-of-view, because such a discharge configuration can be used for a great amount of gas flow volume.

Experiments for the simultaneous removal of NO_x and SO_2 from flue gas using non-thermal plasma based techniques have been performed in various countries [4–9].

The problem of greenhouse gases removal, particularly the reduction of CO_2 from combustion exhaust, using various forms of non-thermal plasma have been studied [10–16].

Experimental

A spontaneously-pulsing, direct-current electric discharge with a ‘brush-like’ streamer to spark transition-type of current pulses, supplied by a d.c. high voltage source was used. The discharge comprises a corona discharge with repeated sparks and surface discharge in the same discharge gap. The individual sparks appeared regularly. As a high-voltage source for this electric discharge, a transformer with ferrite core was used. The repetition frequency of the switching power source was up to 33 kHz. The discharge operates in a corona geometry, but some physical properties correspond to a high-pressure glow discharge. The cathode and anode spots are fully developed in the near electrode region. The discharge has strongly shining channels migrating quickly along the stressed electrode.

For in situ step-by-step time development measurements and material studies, the gas cell corona discharge tube was developed and used (Fig. 1). The discharge system comprises a wire-plane electrode configuration made from various electrode materials (the stressed electrode was 0.2 mm diameter wire wound on glass tube; the non-stressed electrode was a plane 35×100 mm, the inter-electrode distance was 11 mm). The discharge tube was situated inside an IR absorption gas cell so that the electrodes were parallel with the optical axis of the gas cell. A small vacuum system, connected to the gas cell discharge tube enabled various gases to be introduced, to work in defined gas mixtures at atmospheric pressure. The advantage of the system is the possibility of variation of the electrode material. The following materials were tested: duralumin, copper, brass, molybdenum and stainless steel. The gas cell discharge tube was also used for step-by-step kinetic studies. This type of discharge chamber allows in situ IR absorption measurements of the changes induced by the discharge in the steady state regime. The system with the vacuum and the necessary electrical parts is described in Fig. 1.

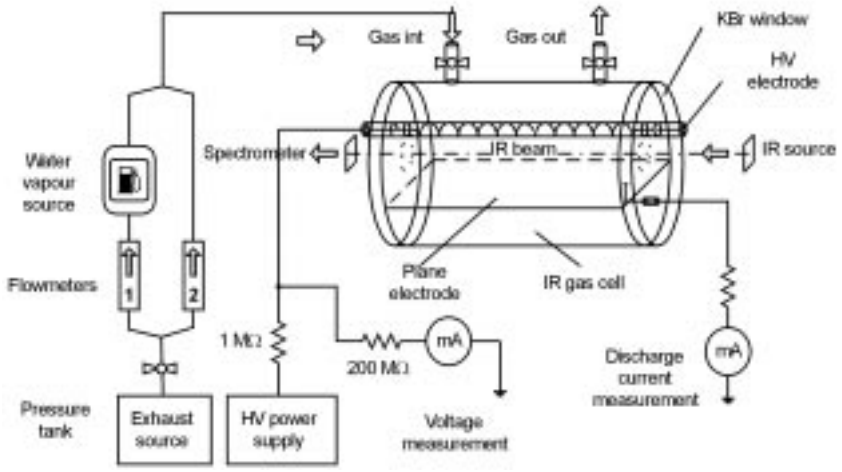

Fig. 1 A gas cell corona discharge tube suitable for material studies and in situ step-by-step time development measurements in the steady state regime

The multifunctional discharge system developed for tests on a pilot scale with a gas flow volume of 50–100 $Nm^3 h^{-1}$ (Fig. 2) comprises 24 discharge tubes connected parallel to each other. One discharge chamber consists of a copper rod with an internal thread (stressed electrode) and coaxial cylinder (non-stressed electrode) with inter-electrode distance of 6 mm. The length of the discharge tube is 50 cm. The synergetic effect of electrode surface catalysis was also present. The reactor was put into the by-pass gas flow or in a full-size exhaust source. A high-voltage dc source of both polarities up to 20 kV, maximum power 500 W and maximum current 30 mA, was applied for discharge generation. An ultrasonic aerosolator was used as source of additional water. On-line diagnostics, using isokinetic sampling, with the sample flows of 30 l min^{-1} before and after the corona reactor, were done by an authorised

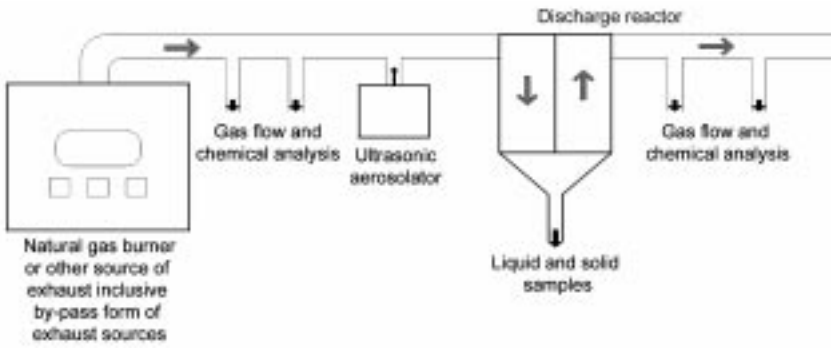

Fig. 2 Schematic diagram of a pilot-scale discharge reactor for a gas flow volume of 50-100 $Nm^3\ h^{-1}$

group of measurers and parallel measurements in our laboratory. The following analysing methods were used: gas chromatography, HPLC, mass spectrometry, total carbon measurement, IR absorption spectrometry, chemiluminiscence, electrochemical methods and magnetic susceptibility (for O_2).

Infrared absorption spectrometry, a powerful method for identification of various materials in gas, liquid and solid phase, was used for regular laboratory analysis in all measurements. Carbon dioxide and carbon monoxide are compounds with intense infrared absorption bands. Due to the action of the electrical plasma, various plasmo-chemical reactions take place. The final reaction products and intermediates are in many cases unknown. The gases were analysed in 10 cm gas cell with KBr, CaF_2 or KRS5 windows of similar construction to the gas cell discharge tube described on Fig. 1.

For solid samples, the KBr pellet technique was used. The sample was mixed with KBr powder in the approximate ratio 0.2–1:100 and pulverised in a vibration mill. The mixture was then pressed under a pressure of 5–22 MPa to form a pellet.

The electrode surface from the discharge system in Fig. 1 was analysed using reflection spectra. The reflection depends on the wavenumber, angle of incidence, index of refraction and absorption features of the sample. The device used allowed measurement of reflection spectra at 20 and 70° angles of incidence. Most of the spectra were measured with a 70° angle.

Results and discussion

Step-by-step kinetic studies made in a gas cell discharge tube

The simplest combustion exhaust can be produced in a gas burner. In our case we used as an exhaust source a measuring calorimeter supplied with methane gas. The gas flow volume from this source varies between 5.5 and 7.6 $dm^3\ min^{-1}$. The residual oxygen in the exhausts was about 12 and nitrogen about 55%. Because NO_x was not present in the exhaust produced, additional NO gas was introduced into the exhaust

from a pressure tank. A part of it was immediately converted into NO_2 and N_2O. Similarly we introduced CO from a pressure tank. The concentrations were estimated by IR absorption spectrometry at the beginning of measurements.

In the case of a positive corona discharge, input exhaust gases contained gas burner exhaust enriched with NO_x and CO to the following concentrations of individual components: CO: 4.5; CO_2: 5.3; NO: 1.7; NO_2: 0.53; H_2O: 15.0%. For N_2O we could not estimate absolute concentrations, but only relative changes.

In the case of a negative corona, input exhaust gases contained gas burner exhaust enriched with NO_x and CO to the following concentrations of individual components: CO: 4.9; CO_2: 8.4; NO: 1.22; NO_2: 0.39; H_2O: 15.4%. As for the positive polarity, for N_2O estimates were made of relative changes of concentrations. The relative decreases in percentage of each component, due to positive and negative corona discharge action, in 2 min intervals, relative to the input concentrations are given in Fig. 3.

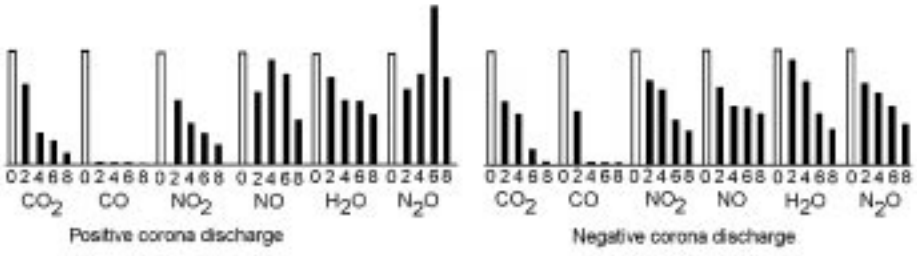

Fig. 3 The time development (in 2 min intervals) of the relative concentrations of enriched gas-burner exhaust components in percentages relative to the input concentrations, due to positive and negative corona discharge action

Another important point is to know how reducing species (residual hydrocarbons, H, CH radicals) influence the time development of products. That was the reason why we did measurements where an oxygen-poor combustion exhaust was generated by slow combustion inside a corona discharge, from a methane – air – NO_x mixture in the gas cell discharge tube. All the introduced air was consumed during the combustion process itself, initiated by the corona discharge and this was not enough for complete combustion (the CO_2, H_2O and NO_2 concentrations were lower, and the CO and NO concentrations higher, than in the case of the combustion calorimeter). No oxygen was present in the combustion exhausts.

For the positive corona discharge, the input concentration of methane was 27, air 72 and NO 1%. The concentrations of exhaust components after 1 min of discharge action were: residual CH_4: 6.6; CO: 9; CO_2: 9.4; NO: 1.11; NO_2: 0.26; H_2O: 10%. The IR spectra of the gas products were scanned in minute intervals up to the 6th min.

For the negative corona discharge, the input concentration of methane was 23.7, air 75.3 and NO 1%. The corona induced combustion process was produced in about the same circumstances. The concentrations of the exhaust components after 1 min of discharge action (corona-induced combustion) were: residual CH_4: 2.4; CO: 6.8;

CO_2: 12.5; NO: 2.2; NO_2: 0.23; H_2O: 10.2%. The IR spectra of the gas products were scanned in minute intervals up to the 5th min.

The relative decreases in percentages of each component, relative to the values reached in the 1st min, are given for both positive and negative polarities in Fig. 4.

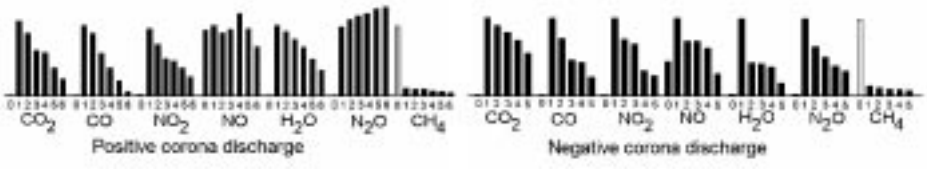

Fig. 4 The time development (in 1 min intervals) of relative concentration changes of each component of a methane–air–NO_x mixture combusted by the discharge, in percentage of the first-min concentration, due to positive and negative corona discharge actions

The basic mixture of CO_2+N_2+H_2O influences the processes initiated by the discharge in the combustion exhaust. To find out more about the time development of product formation, in situ measurements in the gas cell-discharge tube were made. The changes of CO_2 concentration and other typical products in the gas phase are shown in Figs 3 and 4. Here we show the rich variety of new gaseous reaction products and stable radicals formed in the gas phase, especially in positive polarity. The development of these products is based on radicals formed by the discharge, as: –NCO, ON–NCO and OC–NCO in *cis* configuration, $–NH_2$, $–CH_2$ and $–COO^-$. Similar radicals are also formed in rich hydrocarbon flames from nitrogen-containing

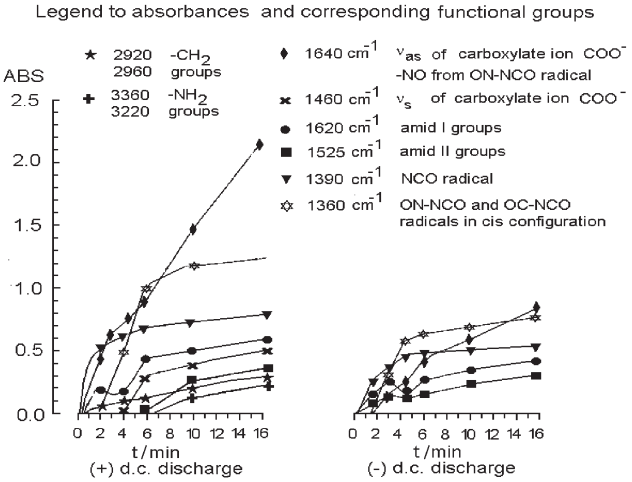

Fig. 5 The time development of products (leading to compounds important in theories of the origin of life) formed in a mixture containing at least CO_2+N_2+H_2O, studied in time steps 0; 1.5; 3; 4.5; 6 and 16 min, for both polarities of discharge. Because the extinction coefficients are unknown, measurements are based on IR absorbances

compounds [17]. On the other hand, the compounds built on the basis of NCO, namely HNCO, are used for quick and effective NO_x removal from combustion exhaust [18]. The time developments of new radicals and products in the gas phase in combustion exhaust mixtures, for both polarities of discharge, are seen from Fig. 5.

A typical feature of our experiments is that the final products are not all gaseous, but solid and/or liquid compounds appearing close to the surface of electrodes. From the gaseous products containing –NCO, ON–NCO, $–COO^-$, CH_2, NH_2 radicals, the surface organometallic compounds, containing amide and amino acid groups, are produced on the electrodes. From thermogravimetric analysis we know that about 95% of the product is a powder from the amorphous amino acid condensate and 5% is an organometallic compound bonded to the surface of the electrode with catalytic properties.

The radicals and clusters produced in the discharge, together with the gaseous products (various amines) are stabilised on the surface of the electrodes, usually by di-, tri-, oligo- or polymerisation and/or cyclisation into heterocyclic compounds producing amino acids and various organometallic compounds on the metal surface. These compounds can be successfully analysed using the KBr pellet technique for powder products and IR reflection spectrometry of the electrode surface. The IR spectra of products from the electrodes confirm the formation of amino acids and heterocyclic unsaturated compounds [19] due to presence of the amide I, II, III bands (wavenumbers 1700–1655, 1565–1400, 1300 cm^{-1}) as seen in Figs 6 and 7. This indicates molecular nitrogen and/or NO_x fixation into the product.

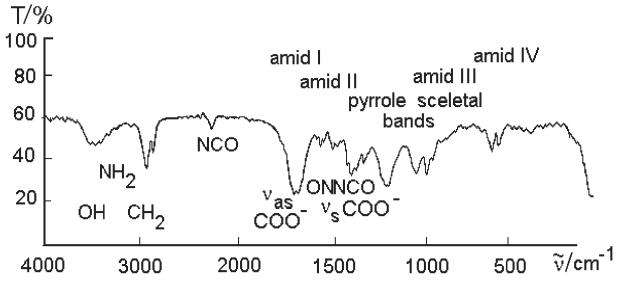

Fig. 6 The IR absorption spectra of the powder product containing amorphous amino acid condensate made using the KBr pellet technique

The product is a statistical polycondensate, containing the amino acids, arginine, lysine, histidine, methionine, glycine alanine, serine, and aspartic acid. This information was obtained by comparing the IR spectra of the product with reference IR absorption spectra of pure components and also from HPLC and thermogravimetric analysis.

The organometallic surface product has important catalytic properties, particularly due to its enhanced dielectric constant. From IR reflection spectra, the presence of oxamidato complexes with known ferroelectric properties [20] and oligo pyrrole type of compounds with probable catalytic activity can be seen. It is known that linear and cyclic tetrapyrrole compounds are important parts of photosyntetic chromophores (linear phycocyanine, cyclic chlorophyl) [21]. Comparison of the IR spectrum

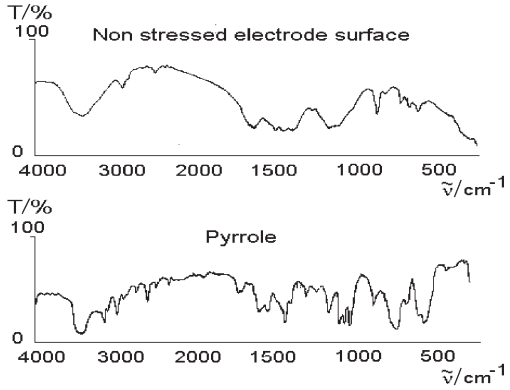

Fig. 7 Comparison of the IR reflection spectrum of a brass metal non-stressed electrode suface containing oxamidato complexes and pyrrole-ring based structures, with the IR spectrum of pyrrole liquid

of the non-stressed electrode surface and the absorption spectrum of liquid pyrrole is shown in Fig. 7.

Pilot-scale measurements

To test the studied processes in real conditions, we have made a group of measurements with the pilot-scale equipment described on Fig. 2. All results from pilot-scale measurements are collected in Fig. 8. Individual types of measurements are selected using legend numbers.

The first test was made on a by-pass from the real exhausts from a stoker-fired brown coal boiler at a heat power plant at Tlmače in Slovakia. The input concentration of CO_2 was about 2%, NO_x was only 40 ppm (the re-circulation of exhaust was used) SO_2 about 300, CO about 500 ppm and O_2 18.5%. The legend for results is No. 1.

In positive discharge polarity and at a flow-rate of about 2 m s^{-1}, the changes of concentration in percentages of the initial concentration, for the individual compounds in order, were the following: (CO_2, O_2, CO, SO_2, NO_x) (–8, +1.1, –27, –79, –62%).

In negative discharge polarity and at a flow-rate of about 2 m s^{-1}, the changes of concentration in percentages of the initial concentration, for the individual compounds in order, were the following: (CO_2, O_2, CO, SO_2, NO_x) (–8, +2, –23, –94, –100%).

From the point-of-view of CO_2, the decrease represents in both cases about 1600 ppm of CO_2. The increase of O_2 was, for the positive corona discharge, about 2035 ppm and, for the negative corona discharge, about 3700 ppm. The residence time was, in both cases, 0.15 s, which seems to be too small.

The second measurement with pilot equipment was done on a full-flow volume of 180 m^3 h^{-1}. The exhaust was from a spark-ignited, petrol-fuelled, Otto-type, internal combustion engine of 1000 cm^3 stroke volume. The analysis of such an exhaust is very complicated because of the dynamic character of the exhaust output. On average, the concentrations of the studied compounds were close to: CO: (0.2–3%); CO_2: (12.5–14%); NO_x: (70–800 ppm); CH_x: (120–500 ppm). The decreases of individual

compounds were very dependent on the applied revolutions, because the equipment used was undersized for the motor (we found this out during the measurements). The efficiency was acceptable only up to 2000 revolutions/min and 50% load of the motor. The measurements were made only for positive polarity of the corona discharge, because the HV source of the discharge system was supplied form the car battery, where the negative pole of the battery is connected to the body of the car. The changes of individual exhaust component concentrations (in percentages of initial concentrations) were, in order: (CO_2, O_2, CO, NO_x, CH_x) [–(20–8); +(200–65); –(66–8); –(58–11); –(0–33)%]. The changes of concentration, in percentages of initial concentrations, for individual compounds and 2000 revolutions/min, are shown in Fig. 8 with legend No. 2. The residence time of exhaust gases in the discharge varies between 0.1 and 0.005 s.

The largest by-pass pilot measurements were made on exhausts from a pulverised-fuel-fired, bituminous coal boiler in a real energy plant at an iron-making factory in

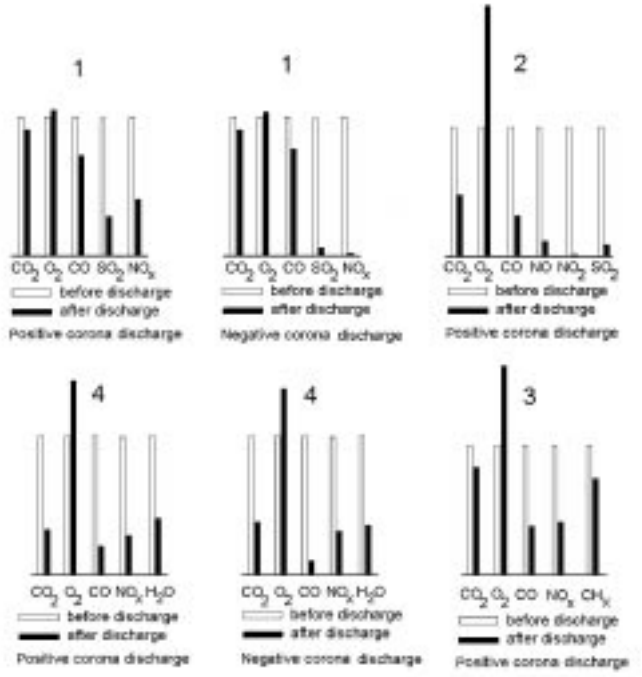

Fig. 8 The changes of concentration in percentages of initial concentrations for exhausts from:
1 stoker-fired, brown coal boiler after action of positive and negative corona discharges
2 spark-ignited, petrol-fuelled, internal combustion engine with 1000 cm^3 stroke volume and revolution of 2000 min^{-1} after positive corona discharge action
3 pulverised-fuel-fired, bituminous coal boiler after action of a positive corona discharge
4 gas-heated, glass oven after action of positive and negative corona discharges

VSZ Košice, Slovakia. The discharge system was built for 200–1000 $Nm^3\ h^{-1}$. The concentration of exhaust components before entering the test equipment varied as follows: CO_2: 2.6–9.2%; NO_x: 120–390 ppm; SO_2: 200–660 ppm; CO: 0–20 ppm and O_2: 10–18%. Measurements were made in a positive polarity discharge. The changes of concentration, in percentages of initial concentrations, for individual compounds in order, were in the following intervals: (CO_2, O_2, CO, NO, NO_2, SO_2) [–(7–100); +(5–90); –(23–90); –(5–92); –(0–100); –(2–92)%]. The residence time varied between 0.05–0.2 s. The concentration changes, in percentages of initial concentrations, for individual compounds are illustrated in Fig. 8 under legend No. 3.

An important test of the studied processes under real conditions was to examine the exhausts from gas-heated glass, because of very high NO_x concentrations. The tests were made on a by-pass of the exhaust from a real gas-heated glass oven for producing of opalescent glass at Desná in the Czech Republic. The measurements are shown in Fig. 8 under legend No. 4.

The input concentrations in positive polarity were CO_2 3.9%, NO_x 1965 ppm, CO 150 ppm and O_2 14.2%, the absolute concentration of H_2O was 5.5%. In positive discharge polarity, the changes of concentration, in percentages of initial concentrations, for individual compounds in order were: (CO_2, O_2, CO, NO_x, H_2O) (–70, +35, –80, –76, –62%).

The input concentrations in negative polarity were CO_2 3.8%, NO_x 2107 ppm, CO 164 ppm and O_2 14.3%, the absolute concentration of H_2O was 5.2%. In negative discharge polarity, the changes of concentration, in percentages of initial concentrations, for individual compounds in order, were: (CO_2, O_2, CO, SO_2, NO_x) (–62.7, +31, –91, –69, –69%).

From the point-of-view of CO_2, the decrease, using positive polarity, represents 2.7% of the absolute CO_2 concentration and, using negative polarity, 2.4% of the absolute CO_2 concentration. The corresponding increases of the absolute O_2 concentration were (positive corona discharge) 4.8% and (in negative polarity) 4.5%. The residence time was in both cases between 0.5–0.6 s.

Conclusions

All the reactions studied took place inside multifunctional equipment working under the non-equilibrium plasma conditions created in an electric discharge. The reactions are strongly influenced by the presence of the high-voltage electric field and heterogeneous catalysis on the electrode surface.

The involved chemistry during final product formation was extracted from step-by-step kinetic studies made inside a gas-cell discharge tube. We have divided the process into three important steps:

- activation,
- formation of energy-rich intermediate species, formation of catalytic spots on the electrode surfaces, volume reactions under non-equilibrium plasma conditions, surface reactions on the electrodes,
- final products and their analysis.

A general overview of the processes taking part in an electric discharge going on in a combustion exhaust is given in Fig. 9.

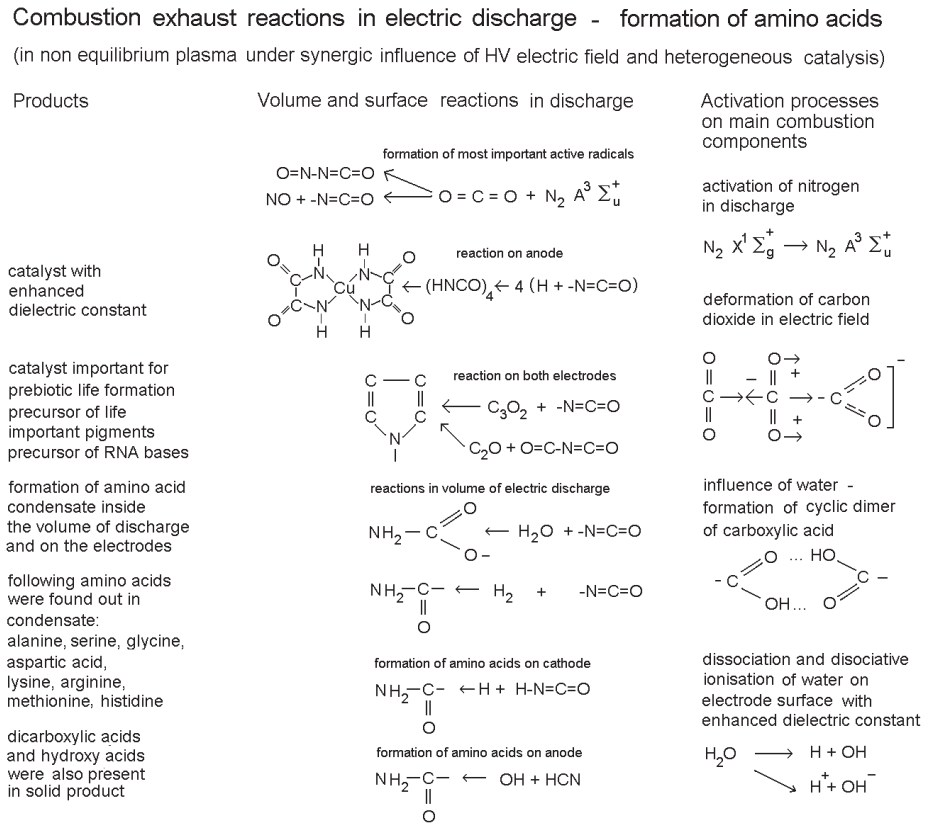

Fig. 9 A general overview of processes taking part in an electric discharge in a combustion exhaust

The most important activation step is the excitation of molecular nitrogen by repeated electron impact in the electric discharge, using a total energy close to 6.5 eV [22].

$$N_2 \quad X^1\Sigma_g^+ \quad \rightarrow \quad N_2\, A^3\Sigma_u^+$$

The electronic state described as $N_2A^3\Sigma_u^+$ has a lifetime between 1.3–1.9 s [22, 23] and that is why it can participate, with a high probability, in chemical reactions. The N_2 activation step is followed by its incorporation into CO_2, to form two of the most important active radicals, namely ON–NCO and –NCO. The development of all further products is based on reaction with NCO (linear amino acids) and ON–NCO (heterocycle-containing amino acids) radicals.

The second important activation step is H_2O dissociation and/or dissociative ionisation on the ferroelectric spots from oxamidato complexes on the electrode.

$$H_2O \rightarrow H + OH \text{ or } H_2O \rightarrow H^+ + OH^-$$

By reaction of –NCO and ON–NCO radicals with water dissociation products, various amino acids and urethanes are formed. Due to the influence of the electric field, CO_2 is deformed into a carboxylate ion. By reaction of the carboxylate ion with water, a cyclic dimer of carboxylic acid is formed and finally dicarboxylic acids (malonic, succinic) and hydroxy acids (apple, citric and tartaric). The urethanes create polyamides, in the case of trimerization, barbituric acid was found in the products. Amino acids can also be formed on both electrodes. Quenching of active species takes place in the electric field inside the drift zone of the discharge and leads to the formation of clusters, and finally polycondensation, of amino acids, together with other products, into amorphous amino acid condensate. The final product of the process is a powder with fractal structure on the microscopic level, with low specific mass and insoluble in water. The main component (95%) of the solid product is amorphous condensate of amino acids, with about 5% of organometallic compounds with catalytic properties. Micrographs of the product are shown in Fig. 10.

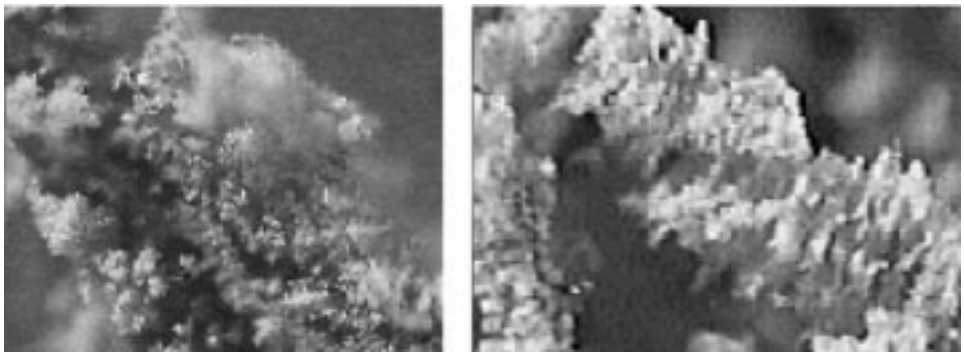

Fig. 10 Micrographs of the amorphous amino acid condensation product

Using liquid chromatography, the following amino acids were found to be present in the condensate: arginine, methionine, histidine and, using IR absorption spectrometry, alanine, serine, glycine, aspartic acid and lysine.

Oxamidato complexes (having enhanced dielectric constants) are the predominant compounds on the anode and participate in the catalytic effects of the anode. The oxamidato complex comprises 4 molecules of HNCO and Cu as the central atom. The reaction with C_3O_2 (decomposition product of $CO_2 \rightarrow CO \rightarrow C_2O \rightarrow C_3O_2$) on the electrode surface in the presence of water, leads to the formation of cyclic tetrapyrrole-ring based products.

Table 1 Collected data from all measurements on a pilot scale to evaulate the changes of CO_2, O_2 and NO_x after electric discharge

Number of test	Discharge polarity	Residence time/s	Input concentrations			Output concentration			Concentration change		
			CO_2/ %	O_2 %	NO_x/ ppm	CO_2/ %	O_2/ %	NO_x/ ppm	$-CO_2$/ %	$+O_2$/ %	$-NO_x$/ ppm
1	Positive	0.15	2	18.5	40	1.84	18.71	15.2	0.16	0.21	24.8
	Negative	0.15	2	18.5	40	1.84	18.87	0	0.16	0.37	40
2	Positive	0.05–0.1	12.5–14	< 2	70–800	10.0–12.1	3.3–6	30–336	1.9–2.5	1.3–4	40.0–464
3	Positive	0.2	5.9	14	260	3.2	20.7	72	2.7	6.7	188
4	Positive	0.6	3.9	14.2	1965	1.2	19	471	2.7	4.8	1494
	Negative	0.6	3.8	14.3	2107	1.4	18.8	659	2.4	4.5	1448

Test numbers
1 stoker-fired, brown coal boiler
2 petrol-fuelled, spark-ignited, Otto internal combustion engine with 1000 cm^3 stroke volume
3 bituminous pulverised smelting boiler
4 gas-heated glass oven

The pyrrole-ring based compounds, which are the bases of life-important pigments (cyclic terapyrrole pigment with central atom Mg=chlorophyll, linear terapyrrole pigment with central atom Cu=phycocyanine, precurzor of RNA basis cytosine and uracyl), are formed on both electrodes.

Pyrrole-ring-containing amino acid histidine and RNA bases such as cytosine and uracyl are also formed on the electrode surface by splitting from the organometallic product.

Similar processes, responsible for the formation of amino acids in strong and medium reducing primitive atmospheres during the origin of life on Earth, were described by Miller [24]. Combustion exhaust is, from the point-of-view of composition, relevant to neutral pre-biotic atmospheres.

Nitrogen fixation participates in the process due to a linear pyrrole-ring based surface catalyst with copper metal. A similar compound (phycocyanin) [21] is present in thylacoids of blue-green algae Spirulina platensis and various types of cyanobacteria where this compound participates in the photosynthesis of amino acids. Oxygen is formed in a similar way to photosynthesis in the multifunctional system (Fig. 8).

The observed carbon utilisation efficiency in the multifunctional discharge systems described above is high (40–65% of CO_2 is utilised). The energy consumption for conversion of 1 m^3 of the gaseous mixture CO_2–N_2–H_2O into amino acid condensate is 2.3-4.7 Wh m^{-3}, i.e. 8.3–16.9 kJ m^{-3}.

The decrease of CO_2 and the increase of O_2 compared to the input values is seen from the data in Table 1. The effect is stronger in positive discharge polarity and depends on the residence time inside the discharge system. We have found out that lengthening of the discharge tube does not lead to a significant increase of the energy input (the effect is caused by the character of the applied discharge, i.e. a migrating repeated spark), but leads to an increase in residence time and reaction efficiency, which corresponds to a decrease of the mean energy used for the conversion.

Final remarks for the practical use of the method and product:

- The continuous conversion of exhaust gases into amino acids does not impose limitations on the energy and industry production and can be successfully used for greenhouse gases limitation and exhaust gas cleaning.
- The final product seems to have possible use as a nitrogen-containing fertiliser.

Final remarks concerning scientific aspects of the results:

- The main component (95%) of the solid product is an amorphous condensate of amino acids with about 5% of an organometallic component with catalytic properties.
- The condensate is built up from the following amino acids: arginine, methionine, histidine, alanine, serine, glycine, aspartic acid and lysine. Amino acids lysine and histidine were according to [24] prepared for the first time from inorganic substances, histidine by splitting from an organometallic surface product. The condensate has the character of statistical proteinoid.
- The anode surface product, oxamidato complexes, can be converted into life important cyclic tetrapyrrole pigments, similar to chlorophyll and/or haemoglobin. Linear tetrapyrrole organometallic compounds with central atom Cu

(observed on both of the electrodes) can possess stereo structures similar to the pigment phycocyanine [21], present in thylacoids of blue green algae Spirulina platensis and various types of cyanobacteria, where this compound participates in nitrogen fixation and in the photosynthesis of amino acids.

References

1 D. R. Huffman, Physics Today, Nov. 1991, p. 22.
2 T. Rosswall, Environ. Sci. Technol., 25 (1991) 567.
3 L. Civitano, Industrial Application of Pulsed Corona Processing to Flue Gas, in Non-Thermal Plasma Techniques for Pollution Control, Eds B. M. Penetrante and S. E. Schultheis, NATO ASI Series, Series G: Ecological Sciences, Vol. 34, Part B, Springer-Verlag, Heidelberg 1993, p. 103–130.
4 I. Gallimberti, Pure Appl. Chem., 60 (1988) 663.
5 A. Mizuno, J. S. Clements and R. H. Davis, IEEE Trans. Ind. Appl.V.IA, 22 (1986) 516.
6 S. Masuda, Pure Appl. Chem., 60 (1988) 727.
7 K. Hensel and M. Morvová, Plasma Physics, 36 (1996) 51.
8 B. M. Penetrante, M. C. Hsiao, B. T. Merritt, G. E. Vogtlin and P. H. Wallman, IEEE Trans. Plasma Sci., 23 (1995) 679.
9 A. Mizuno, A. Chakrabarti and K. Okazaki, in Non-Thermal Plasma Techniques for Pollution Control, (Eds B. M. Penetrante and S. E. Schultheis), NATO ASI Series, Series G: Ecological Sciences, Vol. 34, Part B, Springer-Verlag, Heidelberg 1993, pp. 165–186.
10 B. Eliason, F. G. Simon and W. Egli, Non-Thermal Plasma Techniques for Pollution Control, (Eds B. M. Penetrante and S. E. Schultheis), NATO ASI Series, Series G: Ecological Sciences, Vol. 34, Part B, Springer-Verlag, Heidelberg 1993, pp. 321–337.
11 M. Kurdel and M. Morvová, Czech J. Phys., 47 (1997) 205.
12 M. Higashi, S. Uchida, N. Suzuki and K. Fujii, IEEE. Trans. Plasma Sci., 20 (1992) 1.
13 M. Morvová, I. Morva and F. Hanic, Fourth International Conferencee on Greenhouse Gas Control Technologies, Interlaken 1998, Program and Abstract Book, p. 35.
14 Ichiro Maezono and Jen-Shih Chang, IEEE Trans. Ind. Appl., 26 (1990) 651.
15 H. R. Weiss, Proc. Int. Conf. Plasma Chem., 2 (1985) 383.
16 M. Morvová, J. Phys. D: Appl. Phys., 31 (1998) 1865.
17 D. W. Pershing and J. O. I. Windt, 16th Symposium on Combustion, The Combustion Institute, Pittsburg, PA 1977, p. 389.
18 R. A. Perry and D. L. Siebers, Nature (London), 324 (1986) 657.
19 B. A. Zhubanov, O. V. Agashkin and L. B. Rychina, Atlas of IR spectra of heterocyclic monomers and polymers, Nauka of Kazachstan USR, Alma Ata 1984, p. 147.
20 Ambalangodage Champa Jayasuriya, Shigeru Tasaka and Norihiro Inagaki, Physics Express Letters, J. Phys. D: Appl. Phys., 28 (1995) 1534.
21 A. N. Glaser, Ann. Rev. Microbiol., 36 (1982) 173.
22 A. Lofthus and P. H. Krupenie, J. Phys. Chem. Ref. Data, 6 (1977) 113.
23 L. Magne, G. Cernogora and P. Veis, J. Phys. D: Appl. Phys., 25 (1992) 472.
24 S. L. Miller, in 'Major Events in the History of Life', Ed. J. W. Schopf, Jones&Bartlett, Boston 1992, Chap. 1, pp. 1–28.